Investigations of Interaction of the Main Flow with Root and Tip Leakage Flows in an Axial Turbine Stage by Means of a Source/Sink Approach for a 3D Navier-Stokes Solver

Piotr Lampart Andrzej Gardzilewicz
Institute of Fluid Flow Machinery, Polish Academy of Sciences, Gdansk, Poland
Sergey Yershov Andrey Rusanov
Institute of Mechanical Engineering Problems, Ukrainian National Academy of Sciences, Kharkov, Ukraine

The effect of interaction of the main flow with root and tip leakage flows on the performance of an HP stage of an impulse turbine is studied numerically. The flow in blade-to-blade channels and axial gaps is computed with the aid of a 3D Navier-Stokes solver *FlowER*. The numerical scheme is modified to include the source/sink-type boundary conditions at places at the endwalls referring to design locations of injection of leakage and windage flows into, or their extraction from, the blade-to-blade passage. The turbine stage is computed in three configurations. First, computations are made without tip leakage and windage flows with source/sink slots closed. Second, tip leakage slots are open. Third, both tip leakage and windage flow slots are open, and the obtained flow characteristics including kinetic energy losses in the stage are compared so as to estimate the interaction of the main and leakage flows.

Keywords: axial turbine, high-pressure stage, tip leakage, windage flow, stage losses

INTRODUCTION

Fundamental studies of losses in turbomachinery indicate that, besides giving rise to losses of work, leakage flows contribute to the overall creation of entropy and kinetic energy losses. Some entropy is created in the labyrinth seals and in passages between the fixed and rotating parts of turbomachinery. CFD computations in labyrinth seal geometries enable the evaluation of the entropy creation processes there. CFD-based analysis can minimise the mass flow rates of the tip leakage and improve performance of labyrinth seals. However, unlike for the mass flow rate of the tip leakage that is inherent to the labyrinth seal geometry, most of entropy creation due to tip leakage takes place not in the labyrinth seals but in the blade-to-blade passage downstream of the tip leakage jet re-entry where the injected leakage jet mixes with the main stream. Also most of entropy creation due to windage flows takes place not in the passages between the fixed and rotating parts but in the blade-to-blade passage downstream of the windage jet injection. These effects are of utmost importance in short height blading systems.

At the highest level of simplification, that is in linear superposition of losses from all possible sources, the relative enthalpy losses due to tip and root leakages (referred to isentropic enthalpy drop across the turbine stage) can be assumed equal to the relative mass flow rate of the tip and root leakages (referred to the total mass flow rate of the main flow plus leakages), see Gardzilewicz [1]. However, in real flow situations, say, one percent of the relative leakage mass flow rate can result in one, two, three or even more percent of kinetic energy losses in the stage, mainly depending on the direction of the leakage jet injection. And for short-height blading the relative leakage flow rate (tip and root) can be over five percent, giving rise to say ten or more percent of kinetic energy losses in the stage. Tip leakage and windage flows as mass injections or extractions interact also with secondary flows and separations. It is highly recommended that these phenomena should be investigated and 3D codes for turbomachinery flow prediction should enable modelling of these phenomena.

NUMERICAL METHOD

3D modelling of the entire turbine stage or a group of stages, only inlet and exit conditions assumed, still remains an extremely difficult task. The main difficulty lies in the complexity of turbomachinery geometries, and different aspect ratios and flow scales between the main flow in the blade-to-blade passages, tip leakage over shrouded rotor blades, leakage through stator sealing glands, and windage flows in passages between the fixed and rotating parts of the machinery. A picture of a group of stages for an impulse turbine with indicated directions of the above mentioned streams is presented in Fig. 1.

Received May 15, 2000

NOMENCLATURE

Symbols:

a	speed of sound,
c	absolute velocity,
G	mass flow rate,
h	enthalpy,
I	Riemann invariant,
p	pressure,
s	entropy,
S	entropy function p/ρ^{γ},
u	velocity component,
w	relative velocity.

Greeks:

γ	specific heat ratio,
ρ	density,
ξ	kinetic energy losses,
ξ_1	stator loss,
ξ_2	rotor loss,
ξ_{12}	stage loss without exit velocity,
ξ_{12c}	stage loss with exit velocity.

Subscripts:

0	inlet,
1	stator; behind the stator,
2	rotor; behind the rotor (stage),
n	normal,
R	root leakage,
s, s'	isentropic,
t	tangential,
T	total; tip leakage,
W, W'	windage,
$\pm$	right or left (Riemann invariant)

Definitions of losses:

$$\xi_1 = (h_1 - h_{1s}) / (h_{0T} - h_{1s}) ,$$

$$\xi_2 = (h_2 - h_{2s}) / (h_{1T} - h_{2s}) ,$$

$$\xi_{12} = (h_2 - h_{2s'}) / (h_{0T} - h_{2s'}) ,$$

$$\xi_{12c} = (h_{2T} - h_{2s'}) / (h_{0T} - h_{2s'}) ,$$

Enthalpy-entropy diagram for a turbine stage.

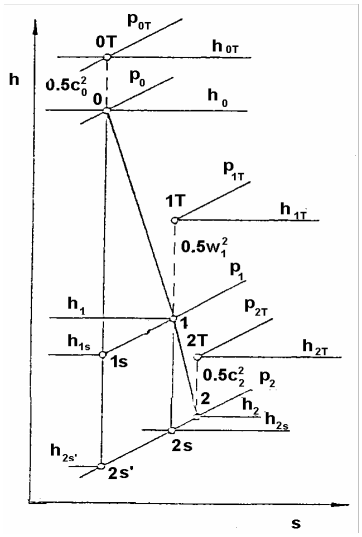

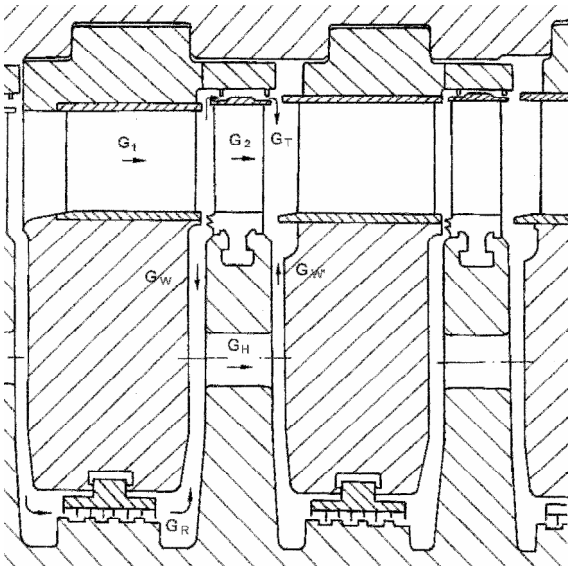

Fig. 1. Impulse turbine geometry.

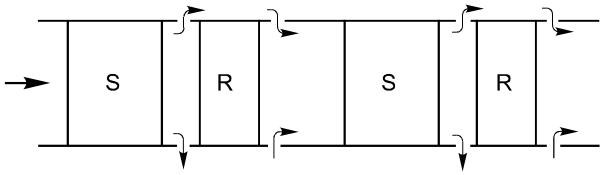

Fig. 2. Computational domain with source/sink-type permeable boundaries to simulate the effect of leakage over shrouded rotor blade tips and windage flows; S - stator, R - rotor.

The computations whose results will be presented in the paper are carried out with the help of a code *FlowER* - solver of viscous compressible multi-stage turbomachinery flows developed by Yershov & Rusanov [2]. The code has been tested on a number of turbomachinery geometries and flow regimes for real full-scale and model turbines, including tests held at the ERCOFTAC Workshops on Turbomachinery Flow Prediction, see Yershov et al. [3]. The main features of the code will shortly be described below.

3D viscous, compressible flow in the blade-to-blade passages and axial gaps is modelled with the help of thin-layer Reynolds-averaged Navier-Stokes equations with a modified Baldwin-Lomax algebraic model of turbulence. The governing equations are solved numerically with the aid of the Godunov-type upwind differencing which does not require artificial diffusion to obtain the convergence of the algorithm, and high resolution ENO scheme for the calculation of convective derivatives, assuring second-order accuracy everywhere in space and time, and third-order accuracy locally. The computational efficiency is increased thanks to the implementation of an implicit step δ of Beam & Warming. The numerical scheme operates on characteristic variables, see Yershov et al. [4].

In addition to boundary conditions typical for turbomachinery codes - a span-wise distribution of the total pressure, total temperature and flow angles at the inlet to the stage; static pressure assumed at the exit; no slip and no heat flux at walls; the assumption of complete spatial periodicity at periodic boundaries upstream of the leading edges and downstream of the trailing edges, combined with the concept of a mixing plane between the fixed and moving blade rows in the steady-state approach, or time-space periodicity and sliding plane in the unsteady approach - source/sink-type boundary conditions are assumed at places at the endwalls referring to design locations of injection of leakage and windage flows into, or their extraction from, the blade-to-blade passage, see Fig. 2. The injection and extraction are accomplished with the application of non-reflective boundary conditions there, giving four values of invariants for injection ($u_n > 0$)

$$I_+ = u_n + 2a / (\gamma - 1) = const ,$$

$$u_{t1} = const , \quad u_{t2} = const , \quad S = p / \rho^{\gamma} = const$$

and one value for extraction ($u_n < 0$)

$$I_- = u_n - 2a/(\gamma - 1) = const$$

where u_n, u_{t1}, u_{t2} are velocity components - one normal and two tangential to the source/sink boundaries, p - pressure, ρ - density, S - entropy function, a - speed of sound, γ - isentropic exponent, I_-, I_+ - left and right Riemann invariant. These invariants can be found, first, from preliminary computations in the basic computational domain without sources and sinks, giving p and ρ at places referring to the source/sink locations, with the density at the sink throat of the tip leakage jet determined from isenthalpic conditions. The corresponding mass flow rates of the injected/extracted fluid - equivalent to the intensity of sources/sinks - can be calculated from more simple 1D studies of leakage and windage flows. Then, the needed velocity components can be obtained based on the density and size of source/sink slots.

The presented approach enables injection of the medium at arbitrary velocities and angles, determination of the effect of mixing of injected medium with the main flow, as well as interaction of injected streams with other vortex flows - secondary flows or separations. Kinetic energy losses in the rotor and stage as defined in Nomenclature are modified to account for leakage streams

$$\xi = \sum_{ex.+s.} \xi_i G_i \; / \sum_{ex.+s.} G_i$$

where the summation extends on all streams that carry away the fluid from the blading system (exit and sinks) and ξ_i is the kinetic energy loss, G_i - mass flow rate in a stream *i*. In the case of nominal directions of leakage and windage flows and equal intensities of respective sources and sinks, the formula reduces to the summation over exit streams only.

NUMERICAL RESULTS

The computed turbine stage is a typical impulse HP stage of a 200MW steam turbine operating at the pressure drop of about 0.9, inlet temperature - 780K, flow rate - 170 kg/s, average reaction - 0.15; the aspect ratios are: span/chord - 0.8 (stator) and 2.0 (rotor), pitch/chord - 0.8, span/diameter - 0.08. Prior to CFD computations, the stage was scrutinised with the aid of a 1D code to evaluate the mass flow rate of the main flow in the blade-to-blade passage of the stator and rotor G_1, G_2 as well as flow rates of leakages at the tip and root G_T, G_R and windage flows G_W, $G_{W'}$ based on the given pressure drops and geometry of labyrinth seals and passages. The results obtained from the 1D approach necessary for further 3D computations are as follows: G_T=*2.7%*G_1, G_W=$G_{W'}$= *1.2%*G_1. Then 3D computations were made in three variants. First, without tip leakage and windage flows with source/sink slots closed, second, with only tip leakage slots open, third, with both tip leakage and windage flow slots open. In source/sink computations, it was assumed by way of example that the fluid is extracted and injected through the sinks and sources in the radial direction (no axial and swirl velocity), which is far from the real turbine situation. However, the computational results presented comparatively below in subsequent Figs. from 3 to 8 can be viewed as an illustration of the described idea of flow solving, showing interesting effects of leakage and windage flows on turbomachinery performance.

The axial distribution of mass flow rate in the rotor computed with source/sink slots closed can be considered nothing more than a measure of convergence of the numerical algorithm. In source/sink computations, sink and source throats belong entirely to the rotor computational domain. In this case, therefore, the axial distribution of mass flow rate in the rotor illustrates the tip leakage mass flow rate equal to 2.7% of the total mass flow (as assumed in the boundary conditions for variant 2), or the summary mass flow rate for tip leakage and windage flows equal to 3.9% of the total mass flow (variant 3) bypassing the rotor blade-to-blade passage and not contributing to the rotor work, see Fig. 3.

Fig. 4 illustrates contours of the entropy function $S=p/\rho^{\gamma}$ in the rotor at pitch-wise subsequent sections between the suction and pressure surface for non-source/sink computations, as well as for source/sink computations with tip leakage and tip leakage plus windage flow. A similar comparison is presented in Fig. 5 with entropy function contours at axially subsequent sections beginning from the leading edge to the trailing edge and downstream into the wake of the rotor. The pictures exhibit characteristic features of subsonic flows in axial turbines. Non-source/sink computations illustrate the development of secondary flows, separation, and wake. The separation and secondary flow vorticity at the root merge towards the mid-span section, giving more loss than that due to secondary flows at the opposite endwall. Computations with the tip leakage (pictures in the centre of Figs. 4 and 5), and both with the tip and root leakages (pictures at the bottom), exhibit an effect of mixing of the leakage stream with the main flow adding to flow losses near the

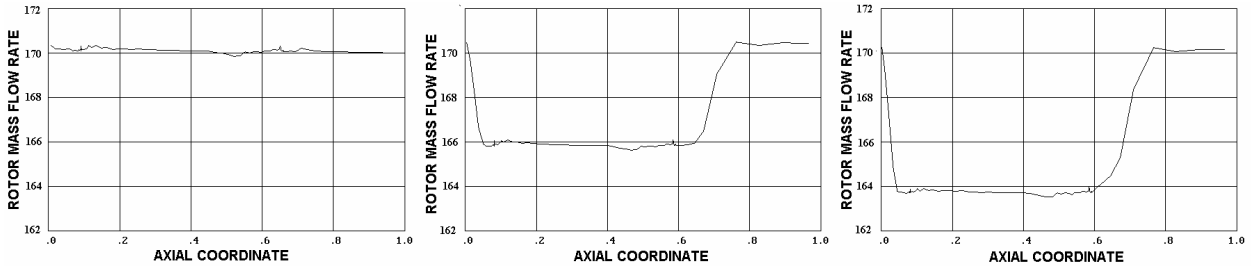

Fig. 3. Axial distribution of mass flow rate in the computational domain of the rotor - computed without sources and sinks (left), computed with tip leakage (centre), computed with tip leakage and windage flows (right).

Fig. 4. Entropy function contours in meridional view in the computational domain of the rotor at 3% (left), 12% (centre left), 48% (centre right) and 96% (right) blade-to-blade distance from the suction surface - computed without sources and sinks (top), computed with tip leakage (centre), computed with tip leakage and windage flows (bottom).

tip endwall, or both at the tip and root endwall, respectively. The zone of mixing due to the tip leakage is seen to extend more significantly in the radial direction, compared to that of the windage flows. The effect of windage flows is of a lesser consequence for the flow downstream of the rotor blades than that of the tip leakage flow due to the fact that its flow rate at the source throat was assumed only $1.2\%G_1$, compared to $2.7\%G_1$ for the tip leakage mass flow rate.

There are also other effects of interaction of tip leakage and windage flows with the main stream. They are connected with the formation and development of secondary flows and separations. As the root sections exhibit separation from the suction surface of the rotor blade, it is easier to observe the effect of leakage flows on the secondary flow formation at the tip endwall. There, with the tip leakage slots open, the high-entropy boundary-layer fluid is sucked out into the sink slot prior to the rotor. And this brings a considerable reduction in the span-wise extension of the secondary flow zone, which can be noticed in Figs. 4 and 5, as well as in Fig. 6 showing velocity vectors at the suction surface of the rotor blades. This also means less loss due to secondary flows, compared to non-source/sink computations.

The interaction of leakage flows with separations seems to proceed in the opposite way. It can be observed in Figs. 4, 5, 6, and also in Fig. 7 showing entropy function contours and velocity vectors in the rotor at 9% of the blade span from the root. Appearance of separation is not obligatory in HP blading systems. If it appears, this is most likely due to the fact that the angle of attack at the blade has been exceeded locally, or, in general, the pitch/chord/stagger angle optimisation and stator/rotor matching may not have been executed with due care. In our case, the shape of separation at the root undergoes changes with the presented computational variants. The separation zone is the smallest for non-source/sink computations. It slightly changes with a tendency to increase in size in computations with tip leakage. Compared to non-source/sink computations, the separation zone significantly extends with the windage flow slots open. This is an effect of flow modification at the root and extraction of the fluid prior to the rotor that reduces the mass flow rate in the rotor blade-to-blade passage and changes the

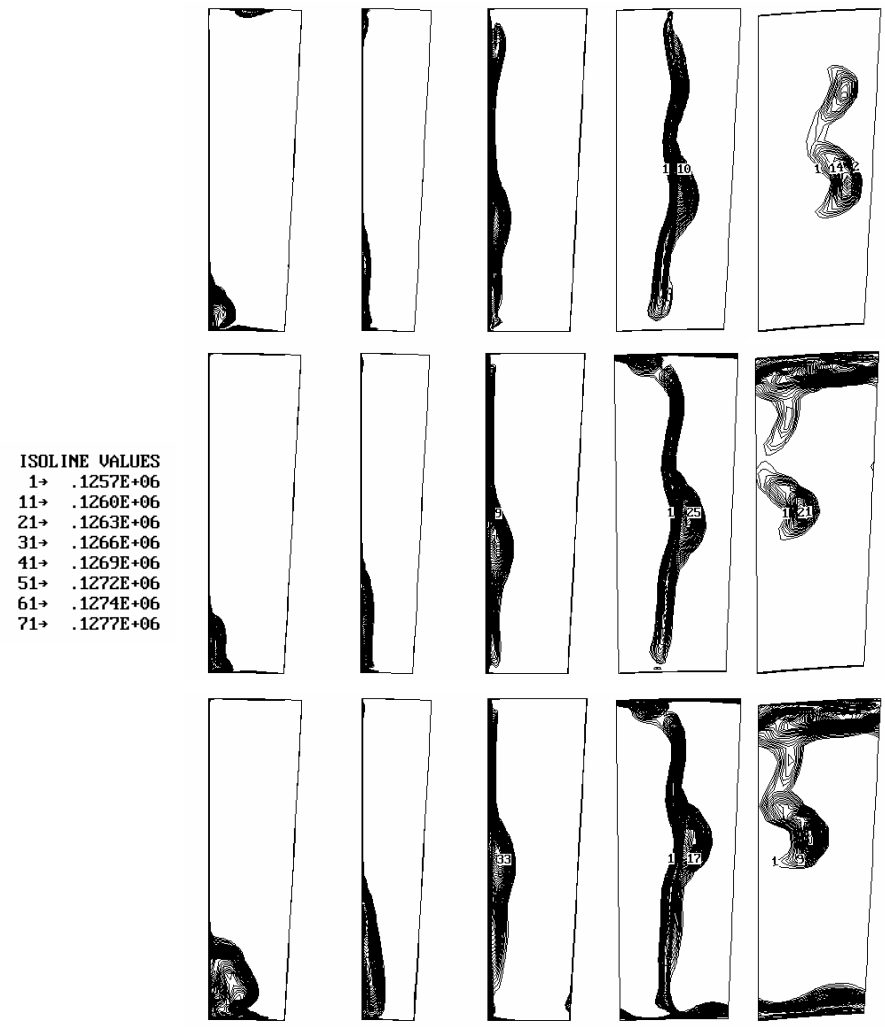

Fig. 5. Entropy function contours in the rotor at 10%, 52%, 96% axial chord from the leading edge, and downstream of the rotor at 10% and 45% axial chord from the trailing edge - computed without sources and sinks (top), computed with tip leakage (centre), computed with tip leakage and windage flows (bottom).

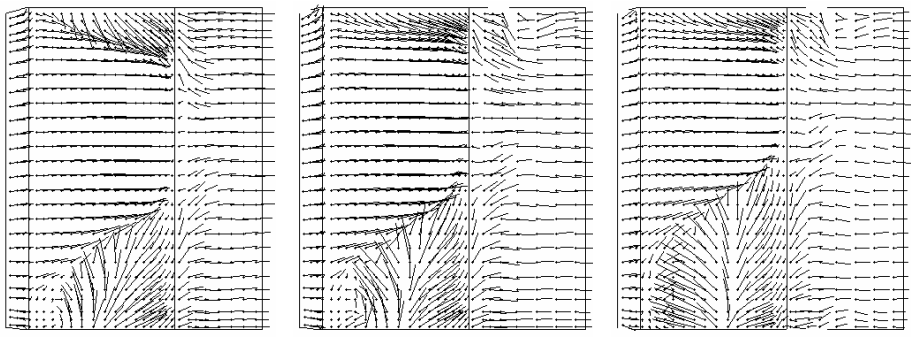

Fig. 6. Velocity vectors in the rotor at the suction surface - computed without sources and sinks (left), computed with tip leakage (centre), computed with tip leakage and windage flows (right).

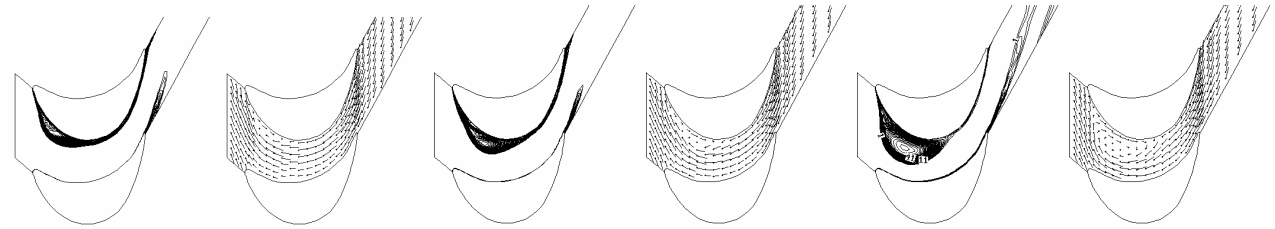

Fig. 7. Entropy function contours and velocity vectors in the rotor at 9% blade span from the root - computed without sources and sinks (left), computed with tip leakage (centre), computed with tip leakage and windage flows (right).

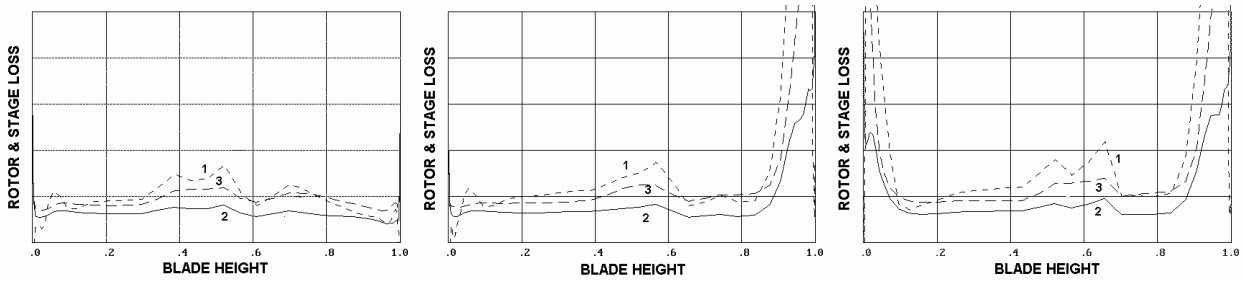

Fig. 8. Span-wise distribution of kinetic energy losses in the rotor (1), stage without the exit velocity (2) and with the exit velocity (3) -computed without sources and sinks (left), computed with tip leakage (centre), computed with tip leakage and windage flows (right).

angle of attack locally.

Fig. 8 is a quantitative reflection of the phenomena observed on previous pictures. The figure shows a comparison of span-wise distribution of kinetic energy losses in the rotor and stage, computed for the three considered variants. The definition of losses can be found in Nomenclature and is easily explained with the help of an enclosed enthalpy-entropy diagram. In all cases the losses are calculated at a section located 42% of the axial chord downstream of the rotor trailing edge. There will certainly be more loss further downstream as the mixing processes are not yet accomplished at the assumed test section. The shape of graphs undergoes considerable redistribution with the considered variants. For non-source/sink computations, similar to pictures of entropy function contours, the maximum at the mid-span is due to the merged root separation and secondary flow vorticity. The second, lower maximum should be attributed to secondary flows at the opposite endwall. Source/sink computations add losses near the endwalls as a result of interaction (mixing) of the injected fluid from the sources with the main stream in the exit diffuser downstream of the rotor trailing edge. Although tip leakage and windage flow losses can not be easily separated from other losses, especially the tip leakage loss is seen to have a great share of the total stage loss. The loss maximum due to separation at the root increases with the increasing mass flow rate by-passing the blade-to-blade passage. The maximum due to secondary flows at the tip is hardly discernible from other sources of loss - this is a decreased rate of secondary flows in source/sink computations.

Compared to non-source/sink computations, stage losses without the exit velocity increase by 2% with only tip leakage slots open and 3% with both tip leakage and windage flow slots open. There is a considerable change in the exit velocity and its radial distribution, which can be deduced from Fig. 8. If the exit velocity is considered a loss, then stage losses with the exit velocity increase by 4% or 5.8%, respectively. If the exit velocity is not necessarily considered a loss, anyway the distribution of the exit velocity in computations with leakages will incur more mixing loss in downstream blade rows.

The presented results are obtained assuming that the medium is extracted and injected through the sinks and sources in the radial direction (no axial and swirl velocity). The investigations will be continued extending on extraction and, especially, injection of tip leakage and windage jets also with axial and swirl velocities according to the geometry of the tip leakage labyrinth seals and windage flow passages. It is expected that the direction of the tip leakage jet re-entry, as well as the angle at which the windage jet is injected have a significant influence on the entropy creation in the downstream mixing process.

CONCLUSIONS

Investigations of the effect of tip leakage over shrouded rotor blades and windage flows on the flow through an HP stage of an impulse turbine have been carried out using a 3D Navier-Stokes code with source/ sink-type permeable boundary conditions implemented at places at the endwalls referring to design locations of injection of leakage and windage flows into, or their extraction from, the blade-to-blade passage. These approach enables tracing and quantitative evaluation of the process of mixing of tip leakage and windage flows with the main stream, and their interaction with secondary flows and separations. The investigations have been conducted for the medium extracted and injected through the sinks and sources in the radial direction with no axial and swirl velocity. The results confirm that the linear superposition of losses and the linear relation between the losses of enthalpy and mass due to leakage flows may not apply in general. More research is required to find the effect of direction of the tip leakage jet re-entry, or the effect of angle at which the windage jet is injected on the entropy creation in the downstream mixing process.

REFERENCES

[1] *Gardzilewicz A.*, Selected problems of computer-aided design of steam turbines and heat cycles, Rep. IFFM, Gdansk, Poland, No. 161, in Polish, (1984).

[2] *Yershov S.V., Rusanov A.V.*, The application package FlowER for the calculation of 3D viscous flows through multistage turbomachinery, Certificate of Ukrainian state agency of copyright and related rights, Kiev, Ukraine, February 19, (1996).

[3] *Yershov S.V., Rusanov A.V., Gardzilewicz A., Badur J., Lampart P.,* Calculations of Test Case 3 - Durham low speed turbine cascade, Test Case 9 - Highly loaded transonic linear turbine guide vane cascade, Proc. V ER-COFTAC Seminar and Workshop on 3D Turbomachinery Flow Prediction, Courchevel, France, January 6-9, (1997).

[4] *Yershov S.V., Rusanov A.V., Gardzilewicz A., Lampart P., Swirydczuk J.,* Numerical simulation of viscous compressible flows in axial turbomachinery, TASK Quarterly, Vol. 2, No. 2, (1998).